Ann. Acad. Rom. Sci.
Ser. Math. Appl.
ISSN 2066-6594 Vol. 6, No. 2/2014

OPTIMAL THICKNESS OF A CYLINDRICAL SHELL*

Paul Ziemann†

Abstract

In this paper an optimization problem for a cylindrical shell is discussed. The aim is to look for an optimal thickness of a shell to minimize the deformation under an applied external force. As a side condition, the volume of the shell has to stay constant during the optimization process. The deflection is calculated using an approach from shell theory. The resulting control-to-state operator is investigated analytically and a corresponding optimal control problem is formulated. Moreover, necessary conditions for an optimal solution are stated and numerical solutions are presented for different examples.

MSC: 49K15, 49J15, 49Q10

keywords: Optimal control of PDE, Shape optimization, Linear elasticity

1 Introduction

In this paper we discuss an optimization problem in linear elasticity, particularly in shape optimization. In this field, much research has been done in the last years. Some few representative books from Sokolowski [1], Pironneau [2], Haslinger [3] and Delfour [4] should be mentioned here.

*Accepted for publication in revised form on September 25-th, 2014

†paul.ziemann@uni-greifswald.de, Ernst-Moritz-Arndt-Universität Greifswald, Institut für Mathematik und Informatik, Walther-Rathenau-Str. 47, D-17487 Greifswald, Germany

In particular, the book from Neittanmaki, Sprekels and Tiba [5] deals with similar problems, though they are using a different model for calculating the deformation. A related problem is also investigated in a paper by Nestler [6], where a simplified (rotational symmetric) case has been handled. That paper was inspired by works from Lepik, Lepikult, Lellep and Schmidt [7, 8, 9, 10].

The task is to look for an optimal thickness of a cylindrical shell to minimize the deformation under an applied external force. In this paper, the stationary case with a loading applied on the shell's midsurface is treated. As an additional restriction, the volume of the shell has to stay constant during the optimization process. Moreover, the thickness should only vary between specified bounds. The deflection is modelled using the "basic shell model" from Chapelle and Bathe [11] which makes use of the Hypothesis from Mindlin and Reissner. As a main result it is shown, that the resulting control-to-state operator is continuous and Gâteaux-differentiable. Followed by this, a corresponding optimal control problem is formulated and necessary conditions for an optimal solution are deduced. Necessary conditions for similar problems can be found e.g. for the rotational symmetric case in [6] and for elastic beams with piecewise constant thickness in [12]; those restrictions are not necessary in this paper. We also investigate the particular numerical implementation of the problem which makes use of an analytically calculated formula for the objective gradient. Finally, numerical solutions for different examples are presented and investigated in relation to the fulfillment of the necessary conditions and convergence properties on refined grids.

2 Geometrical description of the shell

For the geometrical description, we first need a chart describing the midsurface of the shell. Let $\omega \subset \mathbf{R}^2$ be open and connected and $\phi : \overline{\omega} \to \mathbf{R}^3$ be an injective mapping with $\phi \in W^{2,\infty}(\omega)$. We call $\mathbf{S} = \phi(\overline{\omega})$ the midsurface of the shell. We assume that the vectors $a_\alpha := \frac{\partial \phi}{\partial \xi^\alpha}$, $\alpha = 1, 2$ are linearly independent and additionally consider an orthonormal vector $a_3 := \frac{a_1 \times a_2}{\|a_1 \times a_2\|}$. We call a_1, a_2 a covariant basis of the tangent plane of the midsurface and denote the corresponding contravariant basis by a^1, a^2. Moreover, denote by $a_{\alpha\beta} := a_\alpha \cdot a_\beta$, $\alpha, \beta = 1, 2$ the covariant components of the first fundamental form.

In our particular case involving a cylindrical shell, the set ω can be chosen as $\omega = \{(0, L) \times (\psi_a, \psi_b)\}$ and the mapping ϕ is defined as $\phi(\xi^1, \xi^2) = (\xi^1, R\cos\xi^2, R\sin\xi^2)$, where R is the radius of the shell.

We introduce $t : \mathbf{S} \to \mathbf{R}^+$, $t \in C^{0,1}(\mathbf{S})$ as the *thickness* of the shell and suppress the parametrization ϕ in $t \circ \phi : \omega \to \mathbf{R}^+$ when the context is clear. Let us define the 3D-reference domain

$$\Omega_{(t)} := \left\{ (\xi^1, \xi^2, \xi^3) \in \mathbf{R}^3 \mid (\xi^1, \xi^2) \in \omega, \xi^3 \in \left(\frac{-t(\xi^1, \xi^2)}{2}, \frac{t(\xi^1, \xi^2)}{2} \right) \right\} \quad (1)$$

together with the mapping

$$\Phi_{(t)} : \overline{\Omega}_{(t)} \to \mathbf{R}^3, \quad \Phi_{(t)}(\xi^1, \xi^2, \xi^3) = \phi(\xi^1, \xi^2) + \xi^3 a_3. \quad (2)$$

Note that $\Phi_{(t)}$ depends on the parameter t only via its domain, but not on the right hand side. So the thickness parameter is surpressed for Φ and the derived geometrical quantities in the following text.

We call $\mathbf{B}_{(t)} := \Phi(\Omega_{(t)})$ the shell body, see e.g. figure 1. Let us denote the local covariant and contravariant basis with g_i and g^i, $i = 1, 2, 3$ and the covariant and contravariant components of the metric tensor with $g_{ij} = g_i \cdot g_j$, $g^{ij} = g^i \cdot g^j$, $i, j = 1, 2, 3$, resp. Furthermore we assume $t(\xi^1, \xi^2) < 2R$ which is satisfied in general, since for any shell model one assumes that the thickness is much smaller than the principal radii of curvature. In our case, this means $t(\xi^1, \xi^2) \ll R$. Back to our problem, we get

$$\mathbf{B}_{(t)} = \left\{ \begin{pmatrix} \xi^1 \\ (R + \xi^3)\cos(\xi^2) \\ (R + \xi^3)\sin(\xi^2) \end{pmatrix} \mid (\xi^1, \xi^2) \in \omega, \xi^3 \in \left(\frac{-t(\xi^1, \xi^2)}{2}, \frac{t(\xi^1, \xi^2)}{2} \right) \right\} \quad (3)$$

together with the contravariant basis

$$g^1 = \begin{pmatrix} 1 \\ 0 \\ 0 \end{pmatrix}, \quad g^2 = \frac{1}{R + \xi^3} \begin{pmatrix} 0 \\ -\sin(\xi^2) \\ \cos(\xi^2) \end{pmatrix}, \quad g^3 = \begin{pmatrix} 0 \\ \cos(\xi^2) \\ \sin(\xi^2) \end{pmatrix}. \quad (4)$$

The surface and volume element for our shell are given by

$$\begin{aligned} \mathrm{d}S &= \sqrt{a}\, \mathrm{d}\xi^1\, \mathrm{d}\xi^2, & a &= \det(a_{\alpha\beta}) = R^2 \\ \mathrm{d}V &= \sqrt{g}\, \mathrm{d}\xi^1\, \mathrm{d}\xi^2\, \mathrm{d}\xi^3, & g &= \det(g_{mn}) = \sqrt{a}(1 + \tfrac{\xi^3}{R}). \end{aligned} \quad (5)$$

3 Modeling the displacement

We consider a *small* displacement $U : \mathbf{B}_{(t)} \to \mathbf{R}^3$ of the shell body. For modeling we use the Reissner-Mindlin kinematical assumptions which

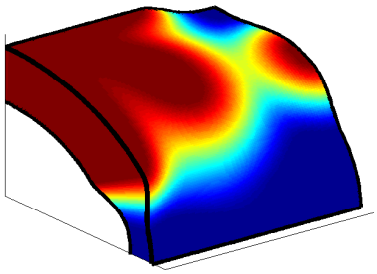

Figure 1: Cylindrical shell with non-constant thickness

state that normals to the midsurface remain straight and unstretched during deformation. This leads to the displacement ansatz

$$U(\xi^1, \xi^2, \xi^3) = u(\xi^1, \xi^2) + \xi^3 \theta(\xi^1, \xi^2) \tag{6}$$

with $u = u_1 a^1 + u_2 a^2 + u_3 a_3$ describing an infinitesimal displacement of all points on a line normal to the midsurface in $\phi(\xi^1, \xi^2)$ and $\theta = \theta_1 a^1 + \theta_2 a^2$ representing a rotation vector. We introduce the space of admissible displacements

$$\mathbf{V} := \left\{(u, \theta) \mid (u_1, u_2) \in H^1(\mathbf{S})^2, u_3 \in H^1(\mathbf{S}), \theta \in H^1(\mathbf{S})^2\right\} \cap \mathbf{BC} \tag{7}$$

where $H^1(\mathbf{S})$ and $H^1(\mathbf{S})^2$ are Sobolev-spaces for scalar functions and first order tensors on the midsurface, resp. Again, we suppress the parametrization in $u \circ \phi$ and $\theta \circ \phi$ defined on ω when the meaning is clear. Let us assume for the boundary conditions **BC** that the shell body is softclamped over the whole boundary $\partial\mathbf{S}$, i.e. $u|_{\partial\mathbf{S}} = 0$. We next consider the linear 3D-Green-Lagrange-strain tensor which is given by

$$e_{ij} = \frac{1}{2}(g_i \cdot U_{,j} + g_j \cdot U_{,i}), \quad i, j = 1, 2, 3, \tag{8}$$

where $U_{,i}$ means the partial derivative of U w.r.t. ξ^i. By Hooke's Law, we get for the components of the stress tensor

$$\sigma^{ij} = \sum_{k,l=1}^{3} H^{ijkl} e_{kl} \tag{9}$$

with $H^{ijkl} = \tilde{L}_1 g^{ij} g^{kl} + \tilde{L}_2 (g^{ik} g^{jl} + g^{il} g^{jk})$ and $\tilde{L}_1$, $\tilde{L}_2$ being the Lamé constants. Using the assumption that the normal stress σ^{33} is zero this simplifies to

$$\begin{aligned} \sigma^{\alpha\beta} &= \sum_{\lambda,\mu=1}^{2} C^{\alpha\beta\lambda\mu} e_{\lambda\mu}, \, C^{\alpha\beta\lambda\mu} = \tfrac{E}{2(1+\nu)} \left(g^{\alpha\lambda} g^{\beta\mu} + g^{\alpha\mu} g^{\beta\lambda} + \tfrac{2\nu}{1-\nu} g^{\alpha\beta} g^{\lambda\mu} \right), \\ \sigma^{\alpha 3} &= \sum_{\lambda=1}^{2} \frac{1}{2} D^{\alpha\lambda} e_{\lambda 3}, \qquad D^{\alpha\lambda} = \tfrac{2E}{1+\nu} g^{\alpha\lambda}, \quad \alpha, \beta = 1, 2, \end{aligned} \tag{10}$$

where E is Young's modulus and ν is Poisson's ratio. Calculating these quantities for our original problem leads to

$$\begin{aligned} \mathbf{e} &:= \begin{pmatrix} e_{11} \\ e_{22} \\ \sqrt{2} e_{12} \end{pmatrix} = \begin{pmatrix} u_{1,1} + \xi^3 \theta_{1,1} \\ u_{2,2} + R u_3 + \xi^3 \left(\theta_{2,2} + \frac{1}{R} u_{2,2} + u_3 \right) + \frac{(\xi^3)^2}{R} \theta_{2,2} \\ \frac{1}{\sqrt{2}} \left(u_{1,2} + u_{2,1} \right) + \frac{\xi^3}{\sqrt{2}} \left(\theta_{1,2} + \theta_{2,1} + \frac{1}{R} u_{2,1} \right) + \frac{(\xi^3)^2}{\sqrt{2} R} \theta_{2,1} \end{pmatrix} \\ \zeta &:= \begin{pmatrix} e_{13} \\ e_{23} \end{pmatrix} = \frac{1}{2} \begin{pmatrix} \theta_1 + u_{3,1} \\ \theta_2 + u_{3,2} - \frac{1}{R} u_2 \end{pmatrix}. \end{aligned} \tag{11}$$

This special vector notation is chosen according to [13] and allows us to rewrite the equilibrium conditions in an elegant way for implementation purposes. Introducing the two-dimensional Lamé-constants

$$L_1 = E \frac{\nu}{(1+\nu)(1-\nu)}, \quad L_2 = \frac{E}{2(1+\nu)} \tag{12}$$

we get for the stress tensor and its matrix representation

$$\begin{aligned} \mathbf{C} &:= \begin{pmatrix} L_1 + 2L_2 & \frac{1}{(R+\xi^3)^2} L_1 & 0 \\ \frac{1}{(R+\xi^3)^2} L_1 & \frac{1}{(R+\xi^3)^4} (L_1 + 2L_2) & 0 \\ 0 & 0 & \frac{2}{(R+\xi^3)^2} L_2 \end{pmatrix} \\ \mathbf{D} &:= \begin{pmatrix} 4L_2 & 0 \\ 0 & \frac{4}{(R+\xi^3)^2} L_2 \end{pmatrix}. \end{aligned} \tag{13}$$

Now consider a force $f \in L^2(\mathbf{S})$ which is applied orthogonal to the mid-surface and formulate the equilibrium conditions for the stationary case

according to the basic shell model from Chapelle and Bathe [11]: Find $(u, \theta) \in \mathbf{V}$ with

$$\begin{aligned} &\int_{\Omega_{(t)}} \sum_{\alpha,\beta,\lambda,\mu=1}^{2} C^{\alpha\beta\lambda\mu} e_{\alpha\beta}(u,\theta) e_{\lambda\mu}(v,\psi) + D^{\alpha\lambda} e_{\alpha 3}(u,\theta) e_{\lambda 3}(v,\psi) \,\mathrm{d}V \\ &= \int_{\omega} f v_3 \,\mathrm{d}S \end{aligned} \tag{14}$$

for all $(v, \psi) \in \mathbf{V}$. We define the bilinear form $A_{(t)}(u, \theta; v, \psi)$ for the left hand side and the linear form $F(v, \psi)$ for the right hand side of (14). The bilinear form can be rewritten using matrix-vector-notation and symmetry properties of the strain and stress tensor as

$$A_{(t)}(u, \theta; v, \psi) = \int_{\Omega_{(t)}} \mathbf{e}^{\mathbf{T}} \mathbf{C} \mathbf{e} + \zeta^T \mathbf{D} \zeta \,\mathrm{d}V. \tag{15}$$

4 Analysis of the model equations

We know from [11] that $A_{(t)}$ is coercive and continuous for fixed t, as well as F is continuous. According to the Lax-Milgram-Lemma there is a unique solution to (14). Therefore the control-to-state operator G which maps the control t to the corresponding displacement (u, θ) is well-defined. Let us define the set

$$U_{\mathrm{reg}} := \{t \in C^{0,1}(\mathbf{S}) \mid 0 < t_{\min} \leq t(\xi^1, \xi^2) \leq t_{\max} < 2R \text{ in } \mathbf{S}\} \tag{16}$$

which is a closed subset of $C^{0,1}(\mathbf{S})$. We now want to investigate the continuity of $G : U_{\mathrm{reg}} \to \mathbf{V}$.

Lemma 1 *For all $t \in U_{\mathrm{reg}}$ the bilinear forms $A_{(t)}$ have a common coercivity constant, i.e.*

$$A_{(t)}(u, \theta; u, \theta) \geq c \,\|(u, \theta)\|_{\mathbf{V}}^2 \quad \forall\, (u, \theta) \in \mathbf{V}. \tag{17}$$

Proof. The proof can easily be derived from the original proof of coercivity in [11].

□

We next consider a sequence $t_n \in U_{\mathrm{reg}}$ that converges strongly to $\bar{t} \in U_{\mathrm{reg}}$ w.r.t. to $\|t\|_{C^{0,1}(\mathbf{S})} = \|t\|_\infty + \mathrm{Lip}(t)$ and denote the corresponding sequence of states by $y_n := (u_n, \theta_n) := G(t_n)$. Using the above Lemma we see that

$$c \,\|(u_n, \theta_n)\|_{\mathbf{V}}^2 \leq A_{(t_n)}(u_n, \theta_n; u_n, \theta_n) = F(u_n, \theta_n) \leq \|f\|_{L^2(\mathbf{S})} \,\|(u_n, \theta_n)\|_{\mathbf{V}}\,, \tag{18}$$

i.e. the sequence y_n is bounded. Hence there is a weakly convergent subsequence, also denoted by y_n, with weak limit $\bar{y} \in \mathbf{V}$.

Lemma 2 *The weak limit $\bar{y}$ is solution of (14) with thickness $\bar{t}$.*

Proof. We first find an alternative form for $A_{(t)}$, namely

$$A_{(t)}(u,\theta;v,\psi) = \int_{\Omega_{(t_{\max})}} \sum_{i,j,k,l=1}^{3} H^{ijkl} e_{ij}(u,\theta) e_{kl}(v,\psi) \chi_{(t)} \,\mathrm{d}V \tag{19}$$

with

$$\chi_{(t)}(\xi^1,\xi^2,\xi^3) := \begin{cases} 1, & \text{if } -\frac{t(\xi^1,\xi^2)}{2} < \xi^3 < \frac{t(\xi^1,\xi^2)}{2} \\ 0, & \text{otherwise} \end{cases} . \tag{20}$$

This can be done since the integrand does not explicitly depend on t and $\chi_{(t)}$ is the characteristic function for $\Omega_{(t)}$. Another expression in terms of the $L^2(\mathbf{B}_{(t_{\max})})$ scalar product for second order tensors is

$$\begin{aligned} A_{(t)}(u,\theta;v,\psi) &= \int_{\Omega_{(t_{\max})}} \langle \sigma(v,\psi)\chi_{(t)}, e(u,\theta)\rangle \,\mathrm{d}V \\ &= \langle \sigma(v,\psi)\chi_{(t)}, e(u,\theta)\rangle_{L^2(\mathbf{B}_{(t_{\max})})}, \end{aligned} \tag{21}$$

where $\sigma(v,\psi)\chi_{(t)}$ has components

$$(\sigma(v,\psi)\chi_{(t)})^{ij} = \sigma(v,\psi)^{ij}\chi_{(t)}. \tag{22}$$

We have $\sigma(v,\psi)\chi_{(t_n)} \to \sigma(v,\psi)\chi_{(\bar{t})}$ in $L^2(\mathbf{B}_{(t_{\max})})$ for fixed $(v,\psi) \in \mathbf{V}$, because

$$\begin{aligned} &\left\|\sigma(v,\psi)\chi_{(t_n)} - \sigma(v,\psi)\chi_{(\bar{t})}\right\|^2_{L^2(\mathbf{B}_{t_{\max}})} \\ &\le \sum_{i,j,k,l=1}^{3} \left| \int_{\Omega_{(t_{\max})}} g_{ik}g_{jl}\sigma^{ij}(v,\psi)\sigma^{kl}(v,\psi)(\chi_{(t_n)} - \chi_{(\bar{t})}) \,\mathrm{d}V \right|. \end{aligned} \tag{23}$$

It holds $\chi_{(t_n)} - \chi_{(\bar{t})} \to 0$ pointwise a.e., so we can conclude

$$g_{ik}g_{jl}\sigma^{ij}(v,\psi)\sigma^{kl}(v,\psi)(\chi_{(t_n)} - \chi_{(\bar{t})}) \to 0 \quad \text{pointwise a.e.} \tag{24}$$

Furthermore $|g_{ik}g_{jl}\sigma^{ij}(v,\psi)\sigma^{kl}(v,\psi)\chi_{(t_{\max})}|$ is an integrable majorant and we get the convergence of the right hand side from (23) to 0. From $(u_n,\theta_n) \rightharpoonup (\bar{u},\bar{\theta})$ in $\mathbf{V}$ it follows that all components and covariant derivatives converge

weakly to the corresponding limit in $L^2(\mathbf{S})$, and so $e(u_n,\theta_n) \rightharpoonup e(\bar{u},\bar{\theta})$ in $L^2(\mathbf{B}_{(t_{\max})})$. We get

$$\langle \sigma(v,\psi)\chi_{(t_n)}, e(u_n,\theta_n)\rangle_{L^2(\mathbf{B}_{(t_{\max})})} \to \langle \sigma(v,\psi)\chi_{(\bar{t})}, e(\bar{u},\bar{\theta})\rangle_{L^2(\mathbf{B}_{(t_{\max})})}, \quad (25)$$

and therefore $F(v,\psi) = \lim\limits_{n\to\infty} A_{(t_n)}(u_n,\theta_n;v,\psi) = A_{(\bar{t})}(\bar{u},\bar{\theta};v,\psi)$.

□

From the uniqueness of the limit $(\bar{u},\bar{\theta})$ we conclude that the whole sequence converges weakly.

Theorem 1 *The convergence of* (u_n,θ_n) *to* $(\bar{u},\bar{\theta})$ *is also strong. Hence the operator* $G : U_{\text{reg}} \to \mathbf{V}$ *is continuous.*

Proof. It holds for $(v,\psi) \in \mathbf{V}$

$$0 = \lim_{n\to\infty} \left(A_{(t_n)}(u_n-\bar{u};\theta_n-\bar{\theta};v,\psi) + A_{(t_n)}(\bar{u},\bar{\theta};v,\psi) - A_{(\bar{t})}(\bar{u},\bar{\theta};v,\psi)\right). \quad (26)$$

We now take $(v,\psi) := (u_n-\bar{u},\theta_n-\bar{\theta})$ and get for the last two terms of (26)

$$\lim_{n\to\infty} \left(A_{(t_n)}(\bar{u},\bar{\theta};u_n-\bar{u},\theta_n-\bar{\theta}) - A_{(\bar{t})}(\bar{u},\bar{\theta};u_n-\bar{u},\theta_n-\bar{\theta})\right) = 0, \quad (27)$$

because

$$\begin{aligned} &\left| A_{(t_n)}(\bar{u},\bar{\theta};u_n-\bar{u},\theta_n-\bar{\theta}) - A_{(\bar{t})}(\bar{u},\bar{\theta};u_n-\bar{u},\theta_n-\bar{\theta})\right| \\ &\le \left| \langle \sigma(\bar{u},\bar{\theta})(\chi_{(t_n)}-\chi_{(\bar{t})}), e(u_n-\bar{u},\theta_n-\bar{\theta})\rangle_{L^2(\mathbf{B}_{(t_{\max})})}\right|. \end{aligned} \quad (28)$$

Analog to the proof of the above Lemma we can show

$$\begin{aligned} \sigma(\bar{u},\bar{\theta})(\chi_{(t_n)}-\chi_{(\bar{t})}) &\to 0 \quad \text{in } L^2(\mathbf{B}_{(t_{\max})}) \\ e(u_n-\bar{u},\theta_n-\bar{\theta}) &\rightharpoonup 0 \quad \text{in } L^2(\mathbf{B}_{(t_{\max})}). \end{aligned} \quad (29)$$

Both statements yield the convergence of the last term from (28) to 0.

From (26) it follows

$$0 = \lim_{n\to\infty} A_{(t_n)}(u_n-\bar{u},\theta_n-\bar{\theta};u_n-\bar{u},\theta_n-\bar{\theta}) \ge \lim_{n\to\infty} c\left\|(u_n-\bar{u},\theta_n-\bar{\theta})\right\|^2_{\mathbf{V}} \ge 0 \quad (30)$$

and therefore the strong convergence $(u_n,\theta_n) \to (\bar{u},\bar{\theta})$ in $\mathbf{V}$. □

Theorem 2 *The control-to-state-operator* $G : U_{\text{reg}} \to \mathbf{V}$ *is Gâteaux-differentiable. For a fixed point* $t \in U_{\text{reg}}$ *with state* $(u_{(t)},\theta_{(t)})$ *and a direction* $q \in C^{0,1}(\mathbf{S})$ *with* $t+\lambda q \in U_{\text{reg}}$ *for all sufficiently small* $\lambda \ge 0$ *it holds* $G'(t)q =$

(r,ρ), where (r,ρ) is the (unique) solution to the variational problem: Find (r,ρ) in $\mathbf{V}$ such that

$$A_{(t)}(r,\rho;v,\psi) = Z_q(v,\psi) \tag{31}$$

holds for all $(v,\psi) \in \mathbf{V}$ where the linear form Z_q is given by

$$Z_q(v,\psi) = -\int_\omega \sum_{\xi_i^3 \in \{\pm\frac{t}{2}\}} \left(\left[\langle \sigma(v,\psi), e(u_{(t)},\theta_{(t)}) \rangle \left(1 + \frac{\xi^3}{R}\right) \right]_{\xi^3=\xi_i^3} \right) \frac{q}{2} \,\mathrm{d}S. \tag{32}$$

Proof. Consider a direction $q \in C^{0,1}(\mathbf{S})$, $0 \leq \lambda \in \mathbf{R}$ as well as $t \in U_{\mathrm{reg}}$ like in the theorem statement. For the solutions $(u_{(t+\lambda q)}, \theta_{(t+\lambda q)})$ and $u_{(t)}, \theta_{(t)}$ of (14) to the thicknesses t and $t+\lambda q$, resp. it holds

$$\begin{aligned} A_{(t)}(u_{(t)},\theta_{(t)};v,\psi) &= F(v,\psi) \\ A_{(t+\lambda q)}(u_{(t+\lambda q)},\theta_{(t+\lambda q)};v,\psi) &= F(v,\psi) \end{aligned} \tag{33}$$

for all (v,ψ) in $\mathbf{V}$. It follows

$$\begin{aligned} 0 &= \frac{1}{\lambda}\left[A_{(t+\lambda q)}(u_{(t+\lambda q)},\theta_{(t+\lambda q)};v,\psi) - A_{(t)}(u_{(t)},\theta_{(t)};v,\psi)\right] \\ &= \int_{\Omega_{(t_{\max})}} \langle \sigma(v,\psi), \frac{e(u_{(t+\lambda q)},\theta_{(t+\lambda q)}) - e(u_{(t)},\theta_{(t)})}{\lambda} \rangle \chi_{(t)} \,\mathrm{d}V \\ &\quad + \int_{\Omega_{(t_{\max})}} \langle \sigma(v,\psi), e(u_{(t+\lambda q)},\theta_{(t+\lambda q)}) \rangle \frac{\chi_{(t+\lambda q)} - \chi_{(t)}}{\lambda} \,\mathrm{d}V. \end{aligned} \tag{34}$$

For the last summand from equation (34) the mapping $Z_\lambda : \mathbf{V} \times \mathbf{V} \to \mathbf{R}$,

$$Z_\lambda(u,\theta;v,\psi) := \int_{\Omega_{(t_{\max})}} \langle \sigma(v,\psi), e(u,\theta) \rangle \frac{\chi_{(t+\lambda q)} - \chi_{(t)}}{\lambda} \,\mathrm{d}V \tag{35}$$

is defined.

Lemma 3 *The limit*

$$-\lim_{\lambda \to 0} Z_\lambda(u_{(t+\lambda q)},\theta_{(t+\lambda q)};v,\psi) =: Z_q(v,\psi) \tag{36}$$

exists and is in $\mathbf{V}^*$.

Proof. It holds that Z_λ can be estimated for fixed λ, because

$$|Z_\lambda(u,\theta;v,\psi)| \leq \frac{1}{\lambda} \int_{\Omega_{(t_{\max})}} |\langle \sigma(v,\psi), e(u,\theta) \rangle| \,\mathrm{d}V \leq \frac{1}{\lambda} C \,\|(v,\psi)\|_{\mathbf{V}} \,\|(u,\theta)\|_{\mathbf{V}}\,. \tag{37}$$

The last inequality comes from the boundedness of $A_{(t_{\max})}$.

We now want to determine the pointwise limit

$$\lim_{\lambda\to 0} Z_\lambda(u,\theta;v,\psi). \tag{38}$$

At first we consider the innermost integral by defining $z : \mathbf{S} \to \mathbf{R}$,

$$z := \int_{-\frac{t_{\max}}{2}}^{\frac{t_{\max}}{2}} \langle \sigma(v,\psi), e(u,\theta)\rangle \frac{\chi_{(t+\lambda q)} - \chi_{(t)}}{\lambda} \sqrt{g}\, \mathrm{d}\xi^3. \tag{39}$$

It holds a.e. in $\mathbf{S}$

$$|z(\xi^1,\xi^2)| \le b(\xi^1,\xi^2) \int_{-\frac{t_{\max}}{2}}^{\frac{t_{\max}}{2}} \left| \frac{\chi_{(t+\lambda q)} - \chi_{(t)}}{\lambda} \right| \mathrm{d}\xi^1 = b(\xi^1,\xi^2)|q(\xi^1,\xi^2)| \tag{40}$$

where $b \in L^1(\mathbf{S})$ because of the boundedness of H^{ijkl} and the polynomial dependence of e_{ij} and $\sqrt{g}$ in ξ^3. So there is an integrable majorant and we can write

$$\begin{aligned} &\lim_{\lambda\to 0} Z_\lambda(u,\theta;v,\psi) = \lim_{\lambda\to 0} \int_\omega \int_{-\frac{t_{\max}}{2}}^{\frac{t_{\max}}{2}} \langle \sigma(v,\psi), e(u,\theta)\rangle \frac{\chi_{(t+\lambda q)} - \chi_{(t)}}{\lambda}\, \mathrm{d}V \\ &= \int_\omega \lim_{\lambda\to 0} \int_{-\frac{t_{\max}}{2}}^{\frac{t_{\max}}{2}} \langle \sigma(v,\psi), e(u,\theta)\rangle \frac{\chi_{(t+\lambda q)} - \chi_{(t)}}{\lambda} (1 + \frac{\xi^3}{R})\, \mathrm{d}\xi^3\, \mathrm{d}S. \end{aligned} \tag{41}$$

Now we investigate the limit

$$\begin{aligned} &\lim_{\lambda\to 0} \int_{-\frac{t_{\max}}{2}}^{\frac{t_{\max}}{2}} f(\xi^3) \frac{\chi_{(t+\lambda q)} - \chi_{(t)}}{\lambda}\, \mathrm{d}\xi^3 \\ &= \lim_{\lambda\to\ 0} \frac{1}{\lambda} \left[\int_{-\frac{(t+\lambda q)}{2}}^{\frac{(t+\lambda q)}{2}} f(\xi^3)\, \mathrm{d}\xi^3 - \int_{-\frac{t}{2}}^{\frac{t}{2}} f(\xi^3)\, \mathrm{d}\xi^3 \right]. \end{aligned} \tag{42}$$

for a continuous function $f \in C([-\frac{t_{\max}}{2}, \frac{t_{\max}}{2}])$. This simplifies to the derivative of the integral bounds with respect to λ at $\lambda = 0$ which evaluates according to Leibniz's formula to

$$\left(f\left(\frac{t}{2}\right) + f\left(-\frac{t}{2}\right) \right) \frac{q}{2}. \tag{43}$$

Therefore, we get

$$\lim_{\lambda\to 0} Z_\lambda(u,\theta;v,\psi) = \int_\omega \sum_{\xi_i^3 \in \{\pm\frac{t}{2}\}} \left(\left[\langle \sigma(v,\psi), e(u,\theta)\rangle (1 + \frac{\xi^3}{R}) \right]_{\xi^3=\xi_i^3} \right) \frac{q}{2}\, \mathrm{d}S. \tag{44}$$

Because of the convergence for fixed (u,θ) and (v,ψ), the mappings Z_λ are uniformly bounded by the Banach-Steinhaus theorem, i.e.

$$Z_\lambda(u,\theta;v,\psi) \leq C \,\|(u,\theta)\|_{\mathbf{V}} \,\|(v,\psi)\|_{\mathbf{V}}\,. \tag{45}$$

Now we want to determine for fixed thickness t and direction q

$$\lim_{\lambda\to 0} Z_\lambda(u_{(t+\lambda q)},\theta_{(t+\lambda q)};v,\psi). \tag{46}$$

It holds

$$\begin{aligned}
&|Z_\lambda(u_{(t+\lambda q)},\theta_{(t+\lambda q)};v,\psi) - Z(u_{(t)},\theta_{(t)};v,\psi)| \\
&\quad\leq\quad |Z_\lambda(u_{(t+\lambda q)}-u_{(t)},\theta_{(t+\lambda q)}-\theta_{(t)};v,\psi)| + |(Z_\lambda - Z)(u_{(t)},\theta_{(t)};v,\psi)| \\
&\quad\leq\quad C\left\|(u_{(t+\lambda q)}-u_{(t)},\theta_{(t+\lambda q)}-\theta_{(t)})\right\|_{\mathbf{V}} \|(v,\psi)\|_{\mathbf{V}} \\
&\qquad\qquad\qquad\qquad + |(Z_\lambda - Z)(u_{(t)},\theta_{(t)};v,\psi)| \\
&\quad\to\quad 0, \quad \lambda\to 0
\end{aligned} \tag{47}$$

Since $(u_{(t)},\theta_{(t)})$ is fixed, we write $Z(v,\psi)$ instead of $Z(u_{(t)},\theta_{(t)};v,\psi)$ and consider from now on Z as a mapping $\mathbf{V}\to\mathbf{R}$. Hence we get

$$\lim_{\lambda\to 0} Z_\lambda(u_{(t+\lambda q)},\theta_{(t+\lambda q)};v,\psi) = Z(v,\psi) \tag{48}$$

with $Z\in\mathbf{V}^*$. To indicate the dependence from the initially chosen q, we finally define

$$Z_q(v,\psi) := -Z(v,\psi) \tag{49}$$

and we get the linear form $Z_q(v,\psi)\in\mathbf{V}^*$.

□

Back to the proof of theorem 2 we again consider equation (34). Because of the linearity of e_{ij} it follows

$$\begin{aligned}
&\int_{\Omega_{(t_{\max})}} \langle\sigma(v,\psi), \frac{e(u_{(t+\lambda q)},\theta_{(t+\lambda q)}) - e(u_{(t)},\theta_{(t)})}{\lambda}\rangle \chi_{(t)}\,\mathrm{d}V \\
&= A_{(t)}\left(\frac{(u_{(t+\lambda q)},\theta_{(t+\lambda q)}) - (u_{(t)},\theta_{(t)})}{\lambda};v,\psi\right).
\end{aligned} \tag{50}$$

By taking the limit in (34) and using the continuity of $A_{(t)}$ we get

$$A_{(t)}\left(\lim_{\lambda\to 0}\frac{(u_{(t+\lambda q)},\theta_{(t+\lambda q)}) - (u_{(t)},\theta_{(t)})}{\lambda};v,\psi\right) = Z_q(v,\psi) \tag{51}$$

for all $(v,\psi) \in \mathbf{V}$. Now we insert $(v,\psi) = \frac{(u_{(t+\lambda q)},\theta_{(t+\lambda q)})-(u_{(t)},\theta_{(t)})}{\lambda}$ in this equation. This yields

$$\begin{aligned} & c \left\| \frac{(u_{(t+\lambda q)},\theta_{(t+\lambda q)}) - (u_{(t)},\theta_{(t)})}{\lambda} \right\|_{\mathbf{V}}^2 \\ & \leq A_{(t)} \left(\tfrac{(u_{(t+\lambda q)},\theta_{(t+\lambda q)})-(u_{(t)},\theta_{(t)})}{\lambda}; \tfrac{(u_{(t+\lambda q)},\theta_{(t+\lambda q)})-(u_{(t)},\theta_{(t)})}{\lambda} \right) \\ & = Z_q \left(\tfrac{(u_{(t+\lambda q)},\theta_{(t+\lambda q)}))-(u_{(t)},\theta_{(t)})}{\lambda} \right) \\ & \leq C \left\| \frac{(u_{(t+\lambda q)},\theta_{(t+\lambda q)}) - (u_{(t)},\theta_{(t)})}{\lambda} \right\|_{\mathbf{V}} \end{aligned} \tag{52}$$

and we see that the sequence $\frac{(u_{(t+\lambda q)},\theta_{(t+\lambda q)})-(u_{(t)},\theta_{(t)})}{\lambda}$ is bounded. Hence, there is a subsequence $\lambda_n \to 0$ such that

$$\frac{(u_{(t+\lambda_n q)},\theta_{(t+\lambda_n q)}) - (u_{(t)},\theta_{(t)})}{\lambda_n} \to (r,\rho), \quad \lambda_n \to 0 \tag{53}$$

weakly in $\mathbf{V}$. Passage to the limit in (51) leads to the variational equation: Find $(r,\rho) \in \mathbf{V}$, such that

$$A_{(t)}(r,\rho;v,\psi) = Z_q(v,\psi) \tag{54}$$

for all $(v,\psi) \in \mathbf{V}$. From the Lax-Milgram-Lemma we know that this equation has a unique solution, so the whole sequence converges to (r,ρ) for $\lambda \to 0$.

□

5 Optimization problem

In this section, the actual optimization problem shall be discussed. In our case the minimization uses the compliance functional, where the deformation is weighted with the incoming force. We state the optimization problem as follows:

$$\begin{aligned} & \min_{t \in C^{0,1}(\mathbf{S}),(u,\theta)\in\mathbf{V}} J(u,\theta;t) := F(u,\theta) + \frac{\lambda}{2} \|t\|^2_{H^1(\mathbf{S})} \\ & \text{s.t. : } A_{(t)}(u,\theta;v,\psi) = F(v,\psi) \quad \forall\,(v,\psi) \in \mathbf{V} \\ & \qquad t_{\min} \leq t(\xi^1,\xi^2) \leq t_{\max} \qquad \text{in } \mathbf{S} \\ & \qquad \int_\omega t \,\mathrm{d}S = C \end{aligned} \tag{55}$$

The constant C represents the volume of the shell and $t_{\min}$, $t_{\max}$ are the lower and upper bound for the thickness, resp. The introduction of a regularization

term was essential for the quality of the numeric solutions. Additionally, we introduce the set

$$U_{\text{ad}} := \{t \in C^{0,1}(\mathbf{S}) \mid t_{\min} \leq t(\xi^1, \xi^2) \leq t_{\max} \text{ in } \mathbf{S}, \int_\omega t \, \mathrm{d}S = C\} \subset U_{\text{reg}}. \tag{56}$$

Note that the set U_{ad} is convex, closed and bounded. By using the control-to-state operator G we can define the reduced objective functional $J_s(t) := J(G(t); t)$ which we will use in this section. The problem (55) can be rewritten in the form

$$\min_{t \in U_{\text{ad}}} J_s(t) = F(G(t)) + \frac{\lambda}{2} \|t\|^2_{H^1(\mathbf{S})} \tag{57}$$

Theorem 3 *Let the set of admissible thicknesses be restricted to*

$$U^M_{\text{ad}} := \{t \in U_{\text{ad}} \mid \text{Lip}(t) < M\} \tag{58}$$

for fixed $M > 0$. Then the problem (57) has at least one solution.

Proof. We know from the Arzela-Ascoli theorem that U^M_{ad} is a closed sequential compact subset of $C(\bar{\omega})$. Moreover, the objective J_s is a composition of continuous mappings. Therefore a minimum exists by the Weierstrass theorem.

□

The aim in this section is to derive necessary conditions for an (locally) optimal solution. As a further result we will also get an expression for the directional derivatives of the objective which is very useful for later numerical calculations. We first define the adjoint state as the solution to:

Find $(p, \eta) \in \mathbf{V}$, such that

$$A_{(t)}(p, \eta; v, \psi) = \nabla_1 J(u, \theta; t)(v, \psi) \tag{59}$$

holds for all $(v, \psi) \in \mathbf{V}$, where $\nabla_1 J(u_0, \theta_0; t_0)$ denotes the Fréchet-derivative of J with respect to (u, θ) at the point $(u_0, \theta_0; t_0)$. We note that because of $\nabla_1 J(u_0, \theta_0; t_0)(v, \psi) = F(v, \psi)$ in our case the adjoint state is equal to the corresponding original state $(u_{(t)}, \theta_{(t)})$.

Theorem 4 *The directional derivative of the reduced objective J_s at point t in direction q is given by*

$$J_s'(t)q = Z_q(u_{(t)}, \theta_{(t)}) + \lambda \langle t, q \rangle_{H^1(\mathbf{S})} = Z_q(G(t)) + \lambda \langle t, q \rangle_{H^1(\mathbf{S})}. \tag{60}$$

Proof. The proof is straightforward by using the chain rule and symmetry of $A_{(t)}$ and can be found e.g. in [5]. The resulting expression then simplifies because of $\nabla_2 J(u_0, \theta_0; t_0)q = \lambda\langle t_0, q\rangle_{H^1(\mathbf{S})}$ and the equality of adjoint and original state.

□

With the help of the directional derivative (60) of the reduced objective we can state necessary conditions for a (locally) optimal solution:

Corollary 1 *Let $t^* \in U_{\mathrm{ad}}$ be a (locally) optimal solution for the problem (55) with corresponding state $(u_{(t^*)}, \theta_{(t^*)})$. Then it holds*

$$J_s'(t^*)(q - t^*) = Z_{(q-t^*)}(u_{(t^*)}, \theta_{(t^*)}) + \lambda\langle t^*, q - t^*\rangle_{H^1(\mathbf{S})} \geq 0 \tag{61}$$

for all directions $q \in U_{\mathrm{ad}}$.

Note, that we need the convexity of U_{ad} for this statement.

6 Numerical implementation

For the numerical solution of the optimization problem a Fortran program was written. The state equation is solved using standard FEM-methods. We use an approach with general shell elements based on biquadratic 9-node Lagrange elements that can be found in [11] or [14]. The finite element displacements are thus given by

$$V_h = \sum_{i=1}^{n} h_i(\xi^1, \xi^2)(v^{(i)} + \xi^3 \eta^{(i)}), \quad \eta^{(i)} \cdot a_3^{(i)} = 0 \tag{62}$$

where $v^{(i)} = (v_1^{(i)}, v_2^{(i)}, v_3^{(i)})^T$, $\eta^{(i)} = (\eta_1^{(i)}, \eta_2^{(i)}, \eta_3^{(i)})^T$, $t^{(i)}$ and $a_3^{(i)}$ denote the translational and rotational displacement components in Cartesian coordinates, the thickness and the unit normal vector at node i, respectively. The h_i are chosen as the shape functions arising from biquadratic ansatz functions λ_j, $j = 1, \ldots, 9$ on the reference element. In local element coordinates, this reads

$$V_h|_E = \sum_{j=1}^{9} \lambda_j(r, s)(v^{(j)} + z\frac{t^{(i)}}{2}\eta^{(i)}). \tag{63}$$

As in (7) we divide into translational and rotational components and consider the finite element displacement space

$$\begin{aligned} \mathbf{V}_h := \{(v_h, \eta_h) \mid v_h = \sum_{i=1}^{n} h_i(\xi^1, \xi^2)v^{(i)}, \eta_h = \pi(\sum_{i=1}^{n} h_i(\xi^1, \xi^2)\eta^{(i)}), \\ \eta^{(i)} \cdot a_3^{(i)} = 0\} \cap \mathbf{BC}, \end{aligned} \tag{64}$$

where π denotes the projection operator onto the tangential plane at point $(\xi^1, \xi^2) \in \mathbf{S}$ and **BC** imposes appropriate boundary conditions on the displacements. Accordingly, the nodal thicknesses $t^{(i)}$ are interpolated using the shape functions h_i which leads to $t_h = \sum_{i=1}^{n} h_i t^{(i)}$. The strain-vector $\mathbf{e}$ is calculated using strain-displacement matrices arising from (11). The matrices $\mathbf{C}$ and $\mathbf{D}$ are calculated using (13) and the value of the discretized bilinear form $A_{(t_h)}(u_h, \theta_h; v_h, \eta_h)$ is obtained using (15) together with Gaussian quadrature. Accordingly, the discretized linear form $F_h(v_h, \eta_h)$ is calculated. We now have to solve: Find $(u_h, \theta_h) \in \mathbf{V}_h$, such that

$$A_{(t_h)}(u_h, \theta_h; v_h, \psi_h) = F_h(v_h, \psi_h) \quad \text{for all } (v_h, \psi_h) \in \mathbf{V}_h. \tag{65}$$

Let the mapping $G_h : \mathbf{R}^n \to \mathbf{V}_h$, $\vec{t} \mapsto (u_h, \theta_h)$ which maps the vector of the nodal thicknesses $\vec{t}$ via the function t_h to the solution of (65) be defined. Finally, the volume constraint is discretized using Gaussian quadrature for t_h over $\mathbf{S}$. We can now state the finite dimensional optimization problem

$$\begin{aligned} \min_{\vec{t} \in \mathbf{R}^n} \; & J_h(\vec{t}) = F_h(G_h(\vec{t})) \\ s.t.: \; & B_h \vec{t} = C \\ & \vec{t}_{\min} \leq \vec{t} \leq \vec{t}_{\max} \end{aligned} \tag{66}$$

where the first constraint represents the volume condition and the second one the pointwise bounds on the thickness.

The linear system arising from (65) is solved using a combination of direct methods (Pardiso solver, see e.g. [15]) and the pcg-method. Namely, the system is solved directly once at the beginning of an iteration of the optimizer, while in the following line search steps the pcg-method is used. As a preconditioner, the LU-factorization obtained from the direct solution does very good work. This combination allows us to benefit from the advantages of both direct and indirect methods.

The actual optimization is done with IpOpt, an Interior-Point algorithm for Large-Scale nonlinear optimization. Here, the expression obtained in (60) for the directional derivative of the objective is used to calculate the gradient of the discrete objective which depends only on the nodal thicknesses. This reduces the running time of the optimizer and raises the accuracy of the solution considerably. The discrete gradient is calculated by evaluating the expression

$$[\nabla J_h(\vec{t})]_i = Z_{h_i}(G_h(\vec{t})) + \lambda \langle t_h, h_i \rangle_{H^1(\mathbf{S})} \tag{67}$$

where we go through all shape functions h_i.

Moreover, we can perform an "optimality test" using equation (61). For a computed solution $\vec{t}^*$ this is done by checking

$$\min_{t \in U_{\text{ad}}} J_s'(t^*)t \stackrel{?}{=} J_s'(t^*)t^*, \tag{68}$$

where the optimization problem can be brought into the discrete form

$$\begin{aligned} \min_{q \in \mathbf{R}^n} \ & \nabla J_h(\vec{t}^*) \cdot q \\ \text{s.t.}: \ & B_h \vec{q} = C \\ & \vec{t}_{\min} \leq \vec{q} \leq \vec{t}_{\max}. \end{aligned} \tag{69}$$

This is a standard linear program with solution $\vec{q}^*$. In general, our numerical solution $\vec{t}^*$ will not be optimal, so there will be a difference $\nabla J_h(\vec{t}^*) \cdot (\vec{q}^* - \vec{t}^*) = -\varepsilon < 0$, where ε is an indicator for the precision of $\vec{t}^*$.

7 Examples

We discuss a part of a tube where different forces are applied on the midsurface. For this, we consider the domain $\omega = (0,1) \times (0, \frac{\pi}{2})$ together with $\phi(\xi^1, \xi^2) = (\xi^1, \cos(\xi^2), \sin(\xi^2))$ to describe the midsurface. We choose $E = 210$ and $\nu = 0.3$ for the material parameters. The minimal and maximal thickness as well as the volume of the shell are chosen as $t_{\min} = 0.05$ and $t_{\max} = 0.15$ and $C = \frac{\pi}{20}$, respectively. This allows us to start with a constant thickness of 0.1 as a feasible initial solution. The regularization parameter λ is chosen in a way that the regularization term is about two to three orders of magnitude smaller than the objective value.

Example 1 We choose a rotational symmetric force $f(\xi^1, \xi^2) = \xi^1(1 - \xi^1)$ which is also symmetric in ξ^1. The corresponding optimal thickness profile over the domain ω is shown in figure 2. We see that the thickness follows approximately the profile of the force and is in particular symmetric in both ξ^1 and ξ^2. The calculation started on a coarse grid and was refined iteratively on finer grids. In the table from figure 2 the differences between the solution on a very fine grid with step-size of 2^{-8} in ξ^1-direction ("exact" solution) and on coarser grids are listed, taken in the max-norm on the particular grid. The step size in ξ^1-direction for each grid is given in the first column. The step-size in ξ^2-direction is chosen to have the same number of nodes. This shows good convergence properties for the thickness when the grid is refined. Moreover, we can see by solution of (69), that the parameter ε in the optimality test can be chosen as $4.5 \cdot 10^{-7}$ which is an indicator for good accuracy of the computed solution t_h^*.

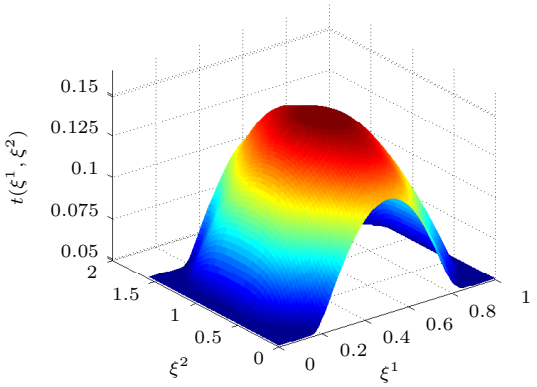

step − size h_{ξ^1}	$\left\|\vec{t}_{\text{ex}} - \vec{t}_h\right\|_\infty$
2^{-4}	$1.16 \cdot 10^{-2}$
2^{-5}	$1.23 \cdot 10^{-3}$
2^{-6}	$9.92 \cdot 10^{-4}$
2^{-7}	$6.87 \cdot 10^{-4}$

Figure 2: Results for example 1, loading $f(\xi^1, \xi^2) = \xi^1(1 - \xi^1)$

Example 2 We choose a periodic force $f(\xi^1, \xi^2) = \sin(2\pi\xi^1)$. The corresponding optimal thickness profile over the domain ω is shown in figure 3. Again, the thickness follows approximately the magnitude of the incoming force. It is noticeable for the first two examples that the optimal thickness does depend on ξ^2 while the incoming force does not. This could be due to the fact that we consider a part of a tube rather than the full tube. The table from figure 3 again shows good convergence properties for smaller step sizes on the grid, though there is a slightly bigger error than in the first example. The parameter ε from (69) can be chosen as $2.37 \cdot 10^{-6}$ which indicates good accuracy of the computed solution.

Example 3 In this example we choose an exponential load $f(\xi^1, \xi^2) = (\exp(\xi^1) - 1)(\exp(\xi^2) - 1)$ which is also asymmetric in ξ^1 and ξ^2. The corresponding optimal thickness profile over the domain ω is shown in figure 4. We see that the thickness is maximal in the region with largest incoming force. But also the two elevations with peaks at $(0.578, 0)$ and $(0, 0.626)$ should be mentioned. The values in the table from figure 4 show the convergence properties on finer grids and the parameter ε from (69) can be chosen as $6.34 \cdot 10^{-6}$ which both indicates good accuracy of the solution.

Example 4 We choose a discontinuous force $f(\xi^1, \xi^2) = 1_{[\frac{1}{4}, \frac{3}{4}] \times [\frac{\pi}{4} - \frac{1}{4}, \frac{\pi}{4} + \frac{1}{4}]}$. The corresponding optimal thickness profile over the domain ω is shown in figure 5. It is noticeable that the optimal thickness is maximal in a region shaped like a cross while the incoming force is applied at a region shaped like

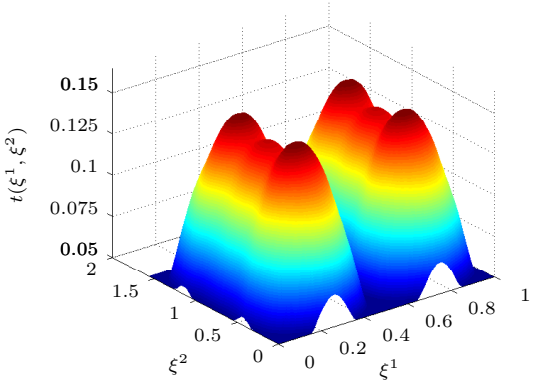

$\text{step} - \text{size}\ h_{\xi^1}$	$\left\|\vec{t}_{\text{ex}} - \vec{t}_h\right\|_\infty$
2^{-4}	$4.22 \cdot 10^{-2}$
2^{-5}	$2.40 \cdot 10^{-2}$
2^{-6}	$7.68 \cdot 10^{-3}$
2^{-7}	$1.55 \cdot 10^{-3}$

Figure 3: Results for example 2, loading $f(\xi^1,\xi^2) = \sin(2\pi\xi^1)$

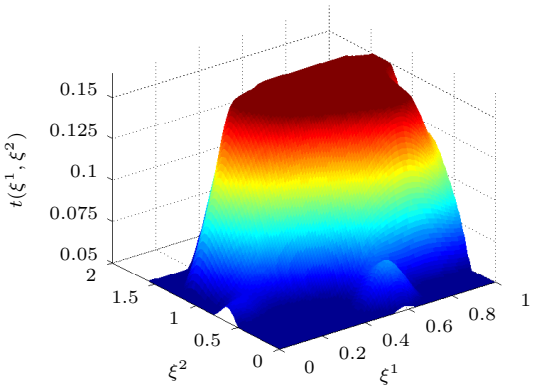

$\text{step} - \text{size}\ h_{\xi^1}$	$\left\|\vec{t}_{\text{ex}} - \vec{t}_h\right\|_\infty$
2^{-4}	$2.48 \cdot 10^{-2}$
2^{-5}	$5.04 \cdot 10^{-3}$
2^{-6}	$1.04 \cdot 10^{-3}$
2^{-7}	$2.12 \cdot 10^{-4}$

Figure 4: Results for example 3, loading $f(\xi^1,\xi^2) = (\exp(\xi^1)-1)(\exp(\xi^2)-1)$

a square, see figure 6. The discontinuity of the incoming force is reflected quite good in the optimal thickness. The table from figure 5 shows similar convergence properties as in the second example. The parameter ε from (69) can be chosen as $3.15 \cdot 10^{-6}$ which indicates good accuracy of the computed solution.

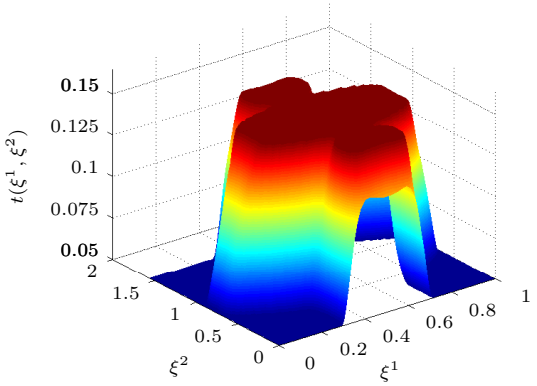

$\text{step} - \text{size } h_{\xi^1}$	$\left\|\vec{t}_{\text{ex}} - \vec{t}_h\right\|_\infty$
2^{-4}	$4.45 \cdot 10^{-2}$
2^{-5}	$1.96 \cdot 10^{-2}$
2^{-6}	$7.04 \cdot 10^{-3}$
2^{-7}	$1.88 \cdot 10^{-3}$

Figure 5: Results for example 4, loading $f(\xi^1, \xi^2) = 1_{[\frac{1}{4}, \frac{3}{4}] \times [\frac{\pi}{4} - \frac{1}{4}, \frac{\pi}{4} + \frac{1}{4}]}$

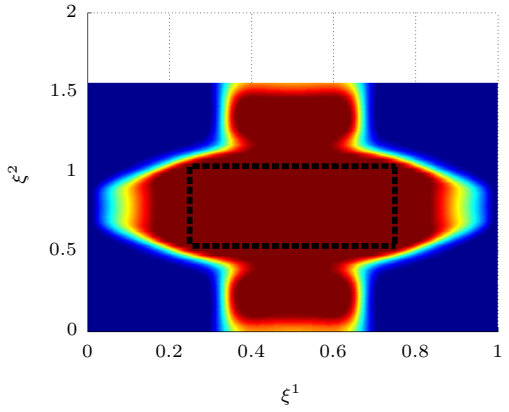

Figure 6: View from above, black line = discontinuity of f

8 Concluding remarks

In this paper we discussed thickness optimization problems for cylindrical shells where the load is applied to the shell's midsurface. In particular we showed the continuity and Gâteaux-differentiability of the control-to-state operator arising from the model equations. The result was used to deduce an expression for the directional derivative of the objective which was the compliance functional in our case. This allowed us to state necessary conditions for an optimal solution. An effective numerical implementation based on direct methods was possible on quite fine grids by using the discretized expression for the directional derivative together with finite element methods. Different examples were investigated where the optimal thickness followed the incoming force in a reasonable way. The computed thicknesses on refined grids showed a good convergence behaviour as well as the evaluation of the necessary conditions indicated good accuracy of the solutions.

References

[1] J. Sokolowski, J.-P. Zolesio. *Introduction to Shape Optimization - Shape Sensitivity Analysis.* Springer Series in Computational Mathematics 16, 1992.

[2] O. Pironneau. *Optimal Shape Design for Elliptic Systems (Scientific Computation).* Springer Verlag, 1983.

[3] J. Haslinger, R. A. E. Mäkinen. *Introduction to Shape Optimization: Theory, Approximation and Computation.* SIAM Philadelphia, 2003.

[4] M. C. Delfour, J.-P. Zolesio. *Shapes and geometries. Analysis, differential calculus and optimization.* SIAM Philadelphia, 2001.

[5] P. Neittanmaki, D. Tiba, J. Sprekels. *Optimization of Elliptic Systems.* Springer, 2006.

[6] P. Nestler. Optimal thickness of a cylindrical shell. *Ann. Acad. Rom. Sci., Ser. Math. Appl.* 4:183–208, 2012.

[7] Ü. Lepik, T. Lepikult. Automated calculation and optimal design of rigid-plastic beams under dynamic loading. *Int. J. Impact Engng.* 6:87–99, 1987.

[8] T. Lepikult, W. Schmidt. Optimal design of rigid-plastic beams subjected to dynamical loading. *Structural Optimization.* 18:116–125, 1999.

[9] J. Lellep. Optimization of inelastic cylindrical shells. *Eng. Optimization.* 29:359–375, 1997.

[10] J. Lellep, P. Nestler, W. Schmidt. Optimization of elastic cylindrical shells. In *Proceedings of the Twenty Second Nordic Seminar on Computional Mechanics.* Aalborg, 2009.

[11] D. Chapelle, K. J. Bathe. *The Finite Element Analysis of Shells - Fundamentals.* Springer, 2003.

[12] V. Azhmyakov and W. Schmidt. On the optimal design of elastic beams. *Struct. Multidisc. Optim.* 27:80–88, 2004.

[13] P. Pedersen. *Elasticity - Anisotropy - Laminates, with matrix formulation, finite elements and an index to matrices.* Solid mechanics, 1998.

[14] P. Lee, K. J. Bathe. Insight into finite element shell discretizations by use of the "basic shell mathematical model". *Computers and Structures.* 83:69–90, 2005.

[15] O. Schenk, K. Gartner, W. Fichtner. Efficient Sparse LU Factorization with Left-right Looking Strategy on Shared Memory Multiprocessors. BIT, 40(1):158-176, 2000.